Analysis of the effectiveness of using complex probing signals to range ambiguity suppression in space monitoring systems

Konstantin Khramov[1*], *Sergey* Zhiganov[1], *Mikhail* Smirnov[1], and *Elena* Zhiganova[1]

[1]Murom Institute of Vladimir State University, 602264 Murom, Russia

Abstract. To improve the range resolution, it is necessary to expand the capture band. However, this leads to range ambiguity interference. This problem is especially serious in space view systems. Therefore, methods of reduction of ambiguity interference are an important part of the information processing system. In modern SAR systems, chirp signals are usually used as probing signals. However, other broadband signals with frequency modulation or PSK signals with different laws of intra-pulse modulation can be used to obtain a radar image. The aim of the work is to analyze the effectiveness of using complex probing signals to reduce range ambiguity interference in space-borne radar systems. In this work, models of radio holograms and radar images of a point target based on chirp signals, signals with hyperbolic and V-shaped frequency modulation are obtained. The results of processing probing chirp signals with pulse-by-pulse change of frequency signs, as well as BPSK signals and ensembles of BPSK signals are also considered.

1 Introduction

In recent decades, space-based remote sensing systems have been actively used in environmental monitoring. Such systems are very often based on the use of SAR which have a number of significant advantages [1-3]. Their performance does not depend on the time of day or the clouds. They allow you to detect objects located under the earth's surface at a shallow depth. Such systems make it possible to form a 3D map of the earth's surface as well. The demand for operational information from remote sensing systems is constantly growing due to the fact that it can be received practically in real time. This information is in demand: in military departments and special services, in agriculture, in maritime transportation management services, in environmental organizations, in geodesy and cartography services, etc. [3-5].

With the development of technology, the requirements for improving the resolution and expanding the shooting band of the scanned surface are increasing. However, at the same time, the negative components of sensing methods are increasing, one of which is the interference of ambiguity in range and azimuth. These interferences arise due to a contradiction in the choice of the frequency of the probing pulses. On the one hand, with an

* Corresponding author: hramovkk@gmail.com

increase in the frequency of repetition, the interference of ambiguity in azimuth decreases, but the interference of ambiguity in range increases, with a decrease in frequency, the opposite effect is observed. In modern SAR, when choosing this parameter, it is assumed that ambiguity interference is minimized either in range or azimuth, while the level of other interference is reduced either structurally and/or algorithmically. In the presented work, the interference of ambiguity in range is considered.

In modern radars, chirp signals are most often used, but signals with other types of frequency and phase modulation have also found applications in radio systems. The aim of the work is to analyze the effectiveness of using probing signals with various types of frequency and phase modulation to suppress range ambiguity interference in space-borne radar systems.

2 Ambiguity interference by range

Let the Earth's surface be probed by a space-borne radar operating in side-view mode. Ambiguity zones are formed along the side lobes of the antenna radiation pattern, as shown in Fig. 1. The speed of the spacecraft, the parameters of the orbit, the parameters of the probing signals and the radiation pattern over the range are known. As a hindrance, we will use reflected signals from the two ambiguity zones closest to the RSA carrier, indicated in Fig. 1 as –1 and +1. In the upper right part of Fig. 1, a dark background schematically shows the signal reflected from the main viewing area, and the pale zones correspond to the signals reflected from –1 and +1 ambiguity zones, which add up to the signal from the main zone.

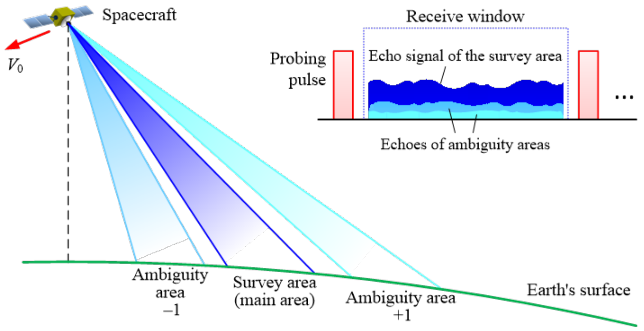

Fig. 1. Illustration of ambiguity by range.

It can be seen from Fig.1 that the range ambiguity signals are formed from reflected pulses received at different points in time. The signal reflected from the target from the viewing area with an inclined range $R(t)$ is the main one, and the signals reflected in the previous and subsequent periods form ambiguity signals. They come along the side lobes of the directional pattern and have values of inclined range

$$R'_n(t) = R(t) + \frac{c \cdot k}{2 \cdot PRF}, \tag{1}$$

where c is the speed of light; PRF is the pulse repetition rate; t is the slow (azimuthal) time; $k = \pm1; \pm2; \pm3...$ is the number of the ambiguity zone.

The main and ambiguous signals are received at the input of the SAR receiver. The total signal can be represented as

$$s(\tau, t) = s_{main}(\tau, t) + \sum_k s_{ambigurity}(\tau, t, k), \tag{2}$$

where τ is the fast time.

It can be seen from Fig. 1 and expression (2) that the main echo signal is added with range ambiguity interference, the power of which depends on the reflectivity and range of objects of ambiguity zones. Moreover, in space-borne systems, due to the large inclined ranges to the sensing area, interference from several ambiguity zones can have a significant effect on the useful signal [6]. When modeling signals reflected from targets in ambiguity zones, it is necessary to take into account the energy of the reflected signal, which depends on the inclined range and the level of the side lobes of the directional pattern.

3 Radar image of a point target forming with chirp signal

We will use the model to process the radio holograms formed by trajectory signals reflected from a standing point object. To do this, we will set the basic survey parameters given in Table 1.

Table 1. SAR parameters.

Parameter	**Value**
Orbit Type	Circular
Orbit Height (km)	650
Mode	Strip
Grazing Angle (degrees)	38
Frequency of Probing(MHz)	9550
Antenna Beamwidth in the range plane (degrees)	20
Losses at the edges of the view field in the range plane (dB)	2
Antenna Beamwidth in the azimuth plane (degrees)	1
Losses at the edges of the view field in the azimuth plane (dB)	0.5
Space resolution (m)	3

Let's consider a model of a radar image from a point target, when a chirp signal was used as a probing signal. The algorithm described in [7] was used to form a radio hologram. Fig. 2 shows the resulting radio hologram of a point object. The term "radio hologram" refers to the value of the samples of the real component of the reflected signal. Here and further, the horizontal axis corresponds to the azimuth values, and the vertical axis corresponds to the range values. The following signal parameters were used in the simulation: duration – 5μs; frequency deviation – 28 MHz, sampling frequency – 42 MHz. The quadrature samples of the signal amplitude were set to 1, and the noise samples were set by the Rayleigh distribution with the parameter $\sigma = 1$ [7].

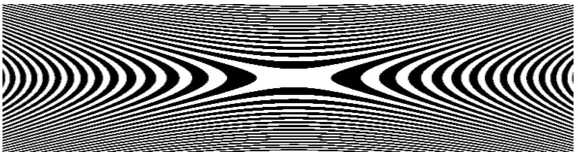

Fig. 2. Radio hologram of a point target forming with chirp signal.

Fig. 3 shows a high-brightness radar image of a point target obtained using a probing chirp signal. The response size at the minus 3 dB level is 5 pixels in azimuth and 3 pixels in range.

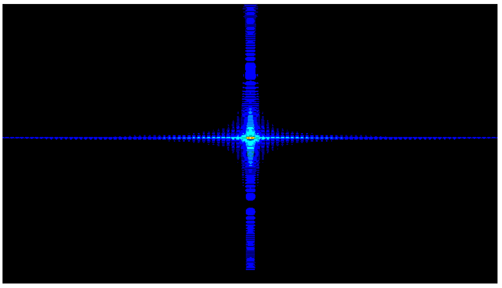

Fig. 3. Radar image of a point target forming with chirp signal.

Range ambiguity interference is generated by bright objects located outside the view field, and distortion of the main signal by interference occurs when the components of the interference signal are superimposed on the corresponding components of the main signal. Fig. 4 shows an example of the overlap of the main and interference signals. The N_p samples of the interference signal are added to the corresponding samples of the main signal. In this case, the N_p can take values from 1 to N.

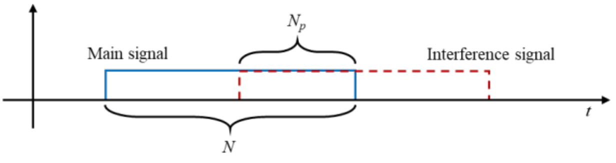

Fig. 4. The location of the main and interference signals by range.

To analyse the effect of range ambiguity interference on radar, consider a situation where there is no signal overlap (N_p=0) and an ambiguous target is in the +1 zone. The reflectivity of an ambiguous target was chosen in such a way that, taking into account the suppression of the radiation pattern over the range, the level of the quadrature components of the interference signal was equal to the level of the main signal. Fig. 5 shows the resulting radio hologram of the main signal and the interference signal. Fig. 5 shows that, even in the case of the same level of signals reflected from the targets from the main area and the ambiguity zone, the holograms differ from each other. This is due to the fact that an ambiguous target has a large inclined range, so the range of Doppler frequencies within the radiation pattern becomes larger and the response of an ambiguous target is defocused.

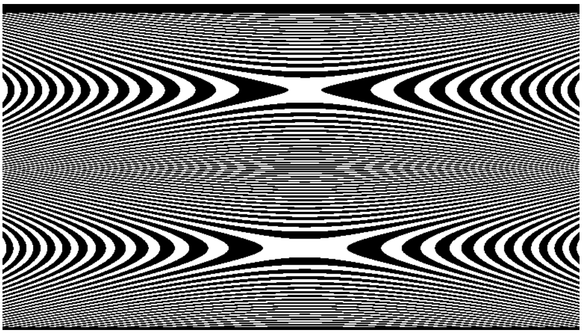

Fig. 5. Radio hologram of a point object in the presence of ambiguity interference (without overlapping signals).

Fig. 6 shows the radar image of the target and the interference point object, the radio hologram of which is shown in Fig. 5. The dimensions of the target remained unchanged, while the size of the interference object is 15 pixels in azimuth and 3 pixels in range.

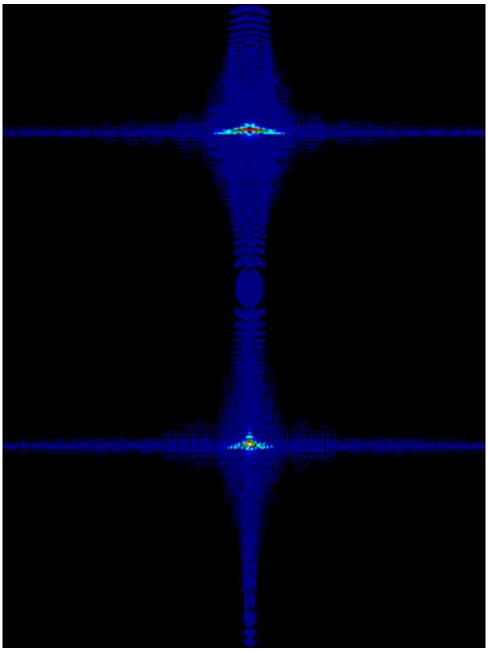

Fig. 6. Radar image of a point object in the presence of interference ambiguity (without overlapping signals).

In the next experiment, the range to the interference object was reduced in such a way that the interference signal was superimposed on half the duration of the main signal, i.e. $N_p=N/2$. Fig. 7 shows the resulting radio hologram, and Fig. 8 shows the corresponding radar image.

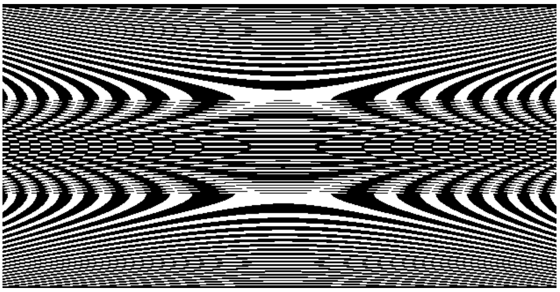

Fig. 7. Radio hologram of a point object in the presence of ambiguity interference (with overlapping signals).

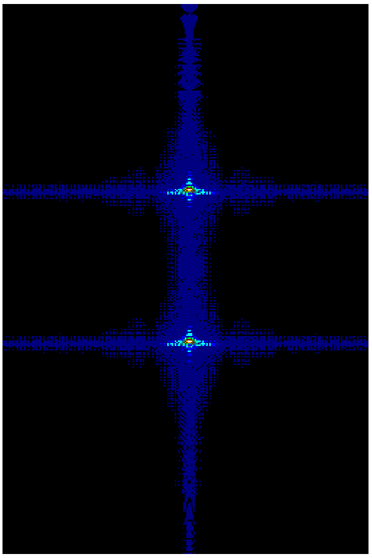

Fig. 8. Radar image of a point object in the presence of interference ambiguity (with overlapping signals).

Fig. 7 shows that in the presence of an ambiguity signal, the hologram is distorted. The target responses and interference to the radar image (Fig. 8) differ significantly from the responses shown in Fig. 6. The main lobe of the target response acquired a rounded shape and its dimensions were 5 pixels in azimuth and 5 pixels in range. In addition, the level of the side lobes in the angular plane has increased. The response of the interference object has also changed due to defocusing. Its level on the radar image is 40 dB less than the target level. Thus, when a range ambiguity interference is applied to the main signal, the resulting target radar is significantly distorted.

4 Radar image of a point target forming with signals with different frequency modulation

In radar, probing broadband signals with different laws of frequency and phase modulation are most often used [8, 9]. Let's perform a simulation of the algorithm for generating a radar image of a point object, when the probing signal is a series of chirp pulses with the same duration and frequency deviation, but with opposite frequency change laws ("up" and "down"). Fig. 9 shows the radar image generated by such probing signals. The main and ambiguous signals overlap each other for half the duration.

Fig. 9 shows that the resulting radar image has a response of the main target, the dimensions of which are 5 pixels in azimuth and 4 pixels in range, as well as interference artifacts of sufficiently high intensity. The noise area has increased in azimuthal coordinate compared to the chirp signal (Fig. 8). The maximum level of the interference signal is -25 dB. Thus, when using such probing signals, which are quasi-orthogonal, it was possible to suppress the level of ambiguity interference in range by 13 dB. Note that the use of chirp signals with the laws of frequency variation "up" and "down" to suppress ambiguity interference in range is effective only for odd ambiguity zones.

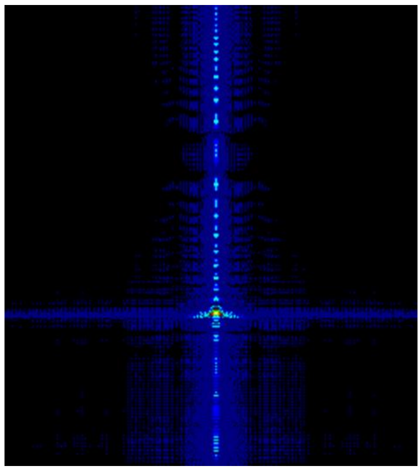

Fig. 9. Radar image of a point object based on chirp signals with opposite frequency variation laws and in the presence of interference ambiguity (with overlapping signals)

Further, a signal with a V-shaped frequency variation law was used as a probe [10]:

$$\Omega(t) = \begin{cases} -\pi W - \mu_v t, -T/2 \le t \le 0, \\ -\pi W + \mu_v t, 0 \le t \le T/2, \end{cases} \quad \omega(t) = \omega_0 + \Omega(t), \quad (3)$$

where ω_0 is the central frequency of the probing signal; W is the frequency deviation; $B=WT$ is the base of the signal; μ is the rate of rise (decline) of the frequency in the pulse, $\mu_v=4\pi W/T$.

Fig. 10 shows a hologram of a point target obtained using the law of frequency variation (3), and Fig. 11 shows a radar image.

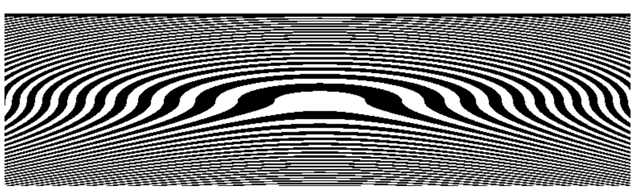

Fig. 10. Radio hologram of a point target forming by signal with a V-shaped frequency law.

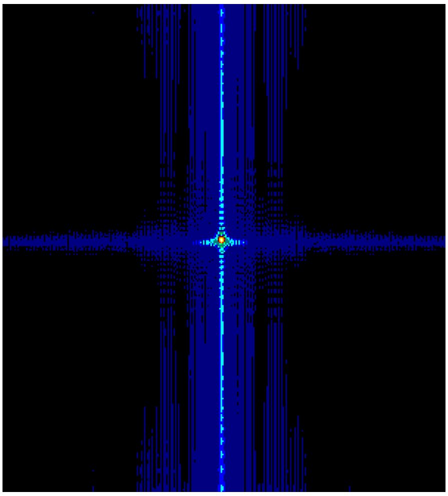

Fig. 11. Radar image of a point target forming by signal with a V-shaped frequency law.

It can be seen from Fig. 10 that with such a law of frequency change, the hologram loses its symmetry horizontally. The radar image, as can be seen from Fig. 11, also differs significantly from the radar image of a point object obtained using a chirp signal. The size of the main lobe of the target response is 5 pixels in azimuth and 5 pixels in range. At the same time, in the azimuthal section φ = 0, within the duration of the probing pulse, the signal level is -25 dB relative to the maximum response. Fig. 11 shows that the quality of the point object formed by the radar is quite low. Fig. 12 shows the radar of a point target in the presence of a range ambiguity interference, obtained for the V-shaped law of frequency variation of the probing signal.

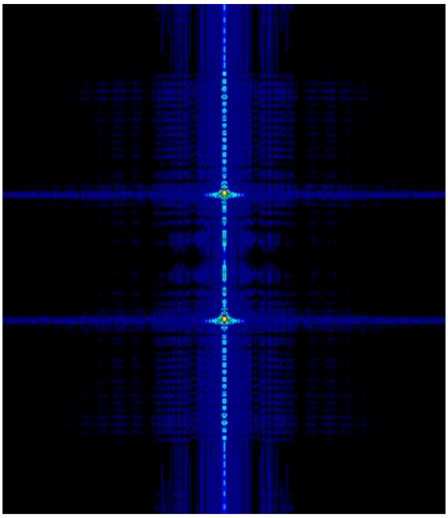

Fig. 12. Radar image of a point object based on chirp signals V-shaped law of frequency variation of the probing signal and in the presence of interference ambiguity (with overlapping signals)

Fig. 12 shows that the level of ambiguity interference turned out to be below the level of the side lobes of the main response.

Next, a signal with a hyperbolic law of frequency variation was considered as a probing signal:

$$\Omega(t) = -\frac{2\pi W}{2} + 2\pi W m \frac{1}{at+b}, \qquad \omega(t) = \omega_0 + \Omega(t), \tag{4}$$

where m is the normalization coefficient.

Fig. 13 shows a hologram of a point target obtained using the hyperbolic law of frequency variation (4), and Fig. 14 shows a radar image

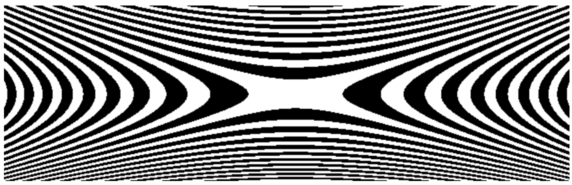

Fig. 13. Radio hologram of a point target forming by signal with a hyperbolic frequency law.

From a comparison of the radio holograms shown in Fig. 2 and Fig. 13 show that they are similar to each other, with a brightly highlighted central area and alternating light and dark stripes radiating symmetrically from the center. Fig. 14 shows that the shape of the point target has changed compared to all previous cases: the azimuth response size was 10 pixels, and the range was 8. The brightness of pixels within this area also varies unevenly. In addition, the side lobes caused by the compression of the signal over the range are significantly larger than in other considered cases.

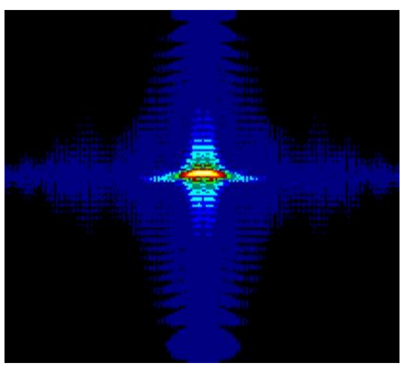

Fig. 14. Radar image of a point target forming by signal with a hyperbolic frequency law.

Figure 15 shows the radar image of a point object in the presence of a range ambiguity interference with the overlap of reflected signals for half the duration. This radar image was obtained using a probing signal with a hyperbolic law of frequency variation. It can be seen from the figure that the shape of the responses of the main target and interference practically does not change.

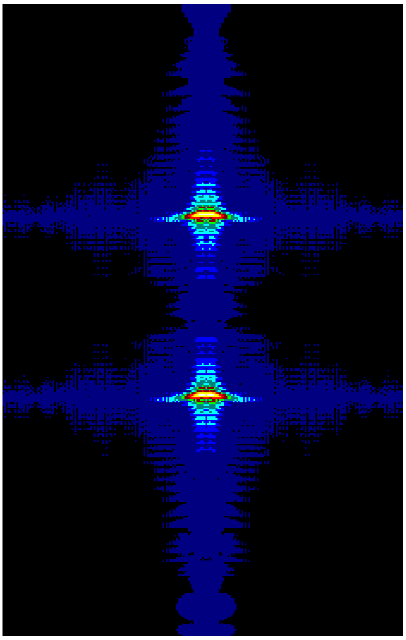

Fig. 15. Radar image of a point object which based on the probing signal with a hyperbolic law of frequency variation and in the presence of interference ambiguity (with overlapping signals)

5 Radar image of a point target when using probing BPSK signals

PSK signals, along with chirp signals, are among the most popular sounding signals in radar technology [10]. These signals are widely used because of the relative simplicity and convenience of formation, as well as good correlation properties.

To form a radar image of a point object, we will use the parameters of the BPSK signal close to the previously analyzed chirp signal, namely: signal duration τ=5μs; signal base B=255, and the generating polynomial for the formation of the M-sequence has the form:

$$f(x) = x^8 + x^6 + x^5 + x^1 + 1.$$

Fig. 16 shows the radio hologram of a point object obtained using the BPSK signal. The object is located in the middle of the range sensing zone.

Fig. 16. Radio hologram of a point target forming by BPSK signal.

From comparing the holograms obtained on the basis of the PSK signal with holograms based on FM signals, it can be seen that they differ significantly from each other. The structure of the quadrature components of the reflected signals when using a probing PSK signal is discrete-rectangular.

One of the distinctive properties of BPSK signals is the possibility of forming ensembles of orthogonal signals of a given duration (Gold, Kasami or Kamaletdinov sequences [10]). Fig. 17 shows a radio hologram of a point object, which is obtained using an ensemble of BPSK signals with the same parameters as in Fig. 16, and obtained using the Gold code with generating polynomials:

$$f_1(x) = x^8 + x^6 + x^5 + x^1 + 1,$$
$$f_2(x) = x^8 + x^7 + x^3 + x^1 + 1.$$

During the simulation, 255 orthogonal BPSK signals were generated, which were sequentially used to form the quadrature components of the reflected signals.

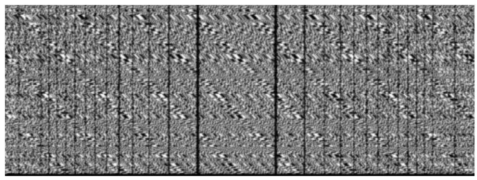

Fig. 17. Radio hologram of a point target forming by ensemble of BPSK signals.

From the comparison of Fig. 16 and Fig. 17, it can be seen that the radio holograms obtained using a single BPSK signal and an ensemble of BPSK signals differ significantly from each other. The structure of the quadrature components of the reflected signals obtained using an ensemble of BPSK signals becomes quite chaotic, unlike a single signal.

Fig. 18 show radar images of a point object. From comparing the images, it can be seen that the images obtained using different probing signals are similar to each other. The size of the target response in both images was 5 pixels in azimuth and 3 pixels in range when using both types of signals.

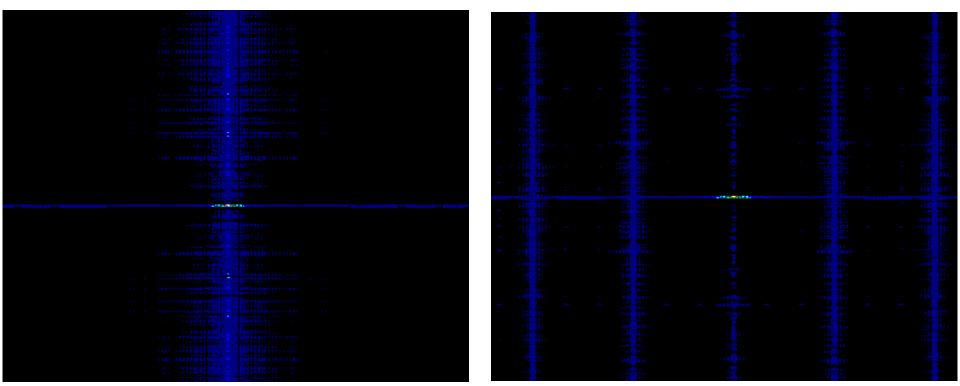

(a) (b)

Fig. 18. Radar image of a point object forming by one BPSK signal (a) and by ensemble of BPSK signals (b)

From the comparison of Fig. 3 and Fig. 18(a), it can be seen that when using the BPSK signal as a probing one, the levels of the side lobes of the range response in its vicinity are significantly lower than the similar level when using the chirp signal. However, at other range values, these levels are significantly higher when using the BPSK signal than when using the chirp signal.

Fig. 19 shows radar images obtained using a single BPSK signal (a) and an ensemble of signals (b) corresponding to the case when the main and interference signals overlap each other for half the duration of the range.

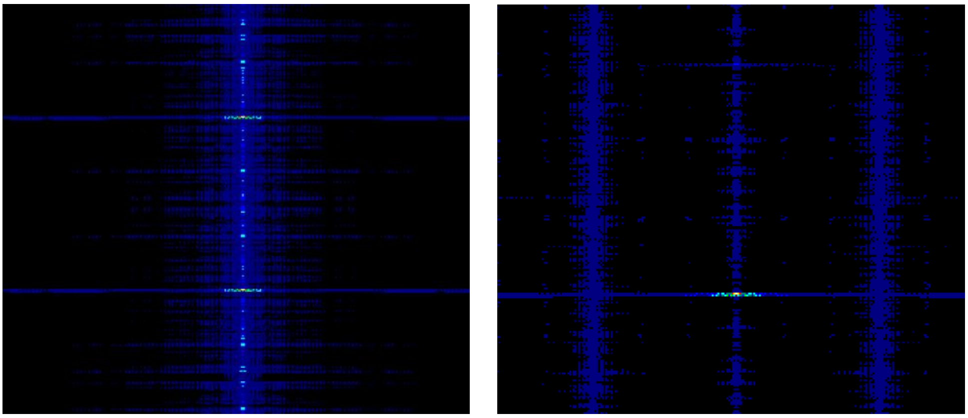

(a) (b)

Fig. 19. Radar image of a point object forming by one BPSK signal (a) and by ensemble of BPSK signals (b) and in the presence of interference ambiguity (with overlapping signals)

From Fig. 19(a) it can be seen that two responses appear in the resulting image – targets and interference. In this case, the size of the target response is 5 pixels in azimuth and 3 pixels in range, and interference is 7 pixels in azimuth and 3 pixels in range. In addition, in the azimuthal section $\varphi = 0$, numerous artefacts appear on the radar image, the level of which reaches -25dB relative to the target response.

As follows from Fig. 19(b), in the case of using an ensemble of BPSK signals, the response level of the ambiguity signal decreases by about 20 dB, while the target response has practically not changed.

6 Conclusion

The paper presents a comparative analysis of holograms and radar images generated in the X-band space-based SAR using complex probing chirp and PSK signals with different laws of intra-pulse modulation under the influence of interference of ambiguity in range.

When modeling a scene containing a point target in the main zone and a point object (interference) in the range ambiguity zone, when using a probing chirp signal, two responses corresponding to the target and interference are observed on the radar image. In this case, the shape and size of the responses in the resulting image are significantly distorted. The response of the interference object turned out to be out of focus.

The use of a sequence of chirp signals with the laws of frequency variation "up" and "down" makes it possible to effectively suppress interference from odd ambiguity zones. As studies have shown, the interference signal on the radar image was suppressed by 13 dB, and the shape of the target response did not change.

When using a signal with a V-shaped frequency law, the target response is not high enough: the level of its side lobes and range is much higher than in the case of using a chirp signal. The presence of range ambiguity interference exacerbates these negative effects on the radar image.

When using a signal with a hyperbolic law of frequency variation, the target response turned out to be blurred in the azimuthal plane. When ambiguity interference appears on the radar image, two of the longest responses in the azimuthal plane are obtained compared to other signals considered.

When using PSK signals, the resulting holograms differ from FM signals and have a discrete rectangular structure. The response of a point target on a radar image has almost the same main lobe as in the case of a chirp signal, regardless of whether a single BPSK signal or an ensemble of such signals was used.

In the presence of range ambiguity interference and the use of a probing BPSK signal on the radar, there are two responses – targets and interference, and the response size of the ambiguity signal in the azimuthal plane is slightly larger than the response of the main target. If an ensemble of BPSK signals is used, the intensity of the ambiguity signal response is reduced by 20 dB.

7 Acknowledgements

The study was supported by the Russian Science Foundation grant No. 23-29-10114.

References

1. D.K. Barton, S.A. Leonov, Radar Technology Encyclopedia (Artech, Boston-London, 1997)
2. Merrill I. Skolnik, Radar Handbook, Third Edition (McGraw-Hill Education, New York, 2008)
3. B. Escalante-Ramirez, Remote Sensing – Applications (Intech, 2012) doi: 10.5772/2670
4. G.R. Curry, Radar system performance modeling (Artech, Norwood, 2005)
5. W. Xu, P. Huang and W. Tan, IEEE Access, **7**, 143780-143791 (2019) doi: 10.1109/ACCESS.2019.2944871.
6. G. Krieger, N. Gebert and A. Moreira, IEEE Geosci. Remote S., **1(4)**, 260-264 (2004) doi: 10.1109/LGRS.2004.832700.
7. K. Khramov and V. Kostrov, E3S Web Conf., **431**, 02026 (2023) https://doi.org/10.1051/e3sconf/202343102026
8. H. Wang, Y. Zhang, J. Xu, G. Liao, C. Zeng, Signal Processing, **168**, 107323 (2020) https://doi.org/10.1016/j.sigpro.2019.107323
9. K. Khramov, S. Zhiganov and M. Smirnov, *Choosing Sets of BPSK-Signals Based on Cycle Sequences for Low Orbit SAR with Multibeam Antenna Array*, in Proceedings of the 26th International Conference on Digital Signal Processing and its Applications (DSPA), Moscow, Russia (2024) doi: 10.1109/DSPA60853.2024.10510096.
10. N. Levanon, E. Mozeson, Radar signals (John Wiley & Sons, 2004)